AN EFFICIENT APPROACH TO BUILDING SUPERSTRUCTURE RECONSTRUCTION USING DIGITAL ELEVATION MAPS

F. Dornaika [1] and M. Brédif [1,2]

[1] Institut Géographique National, MATIS, 2/4 avenue Pasteur, 94165 Saint-Mandé, Cedex, France
[2] Institut TELECOM - TELECOM ParisTech, LTCI UMR 5141 - CNRS, 46 rue Barrault, 75013 Paris, France

KEY WORDS: Building modeling, Digital Elevation Map, model-based reconstruction, parameter fitting, building superstructure

ABSTRACT:

This paper describes an efficient method for detecting and modeling roof superstructures (detailed volumes present on roofs such as chimneys, dormer windows...) using only a Digital Elevation Map (DEM) and an initial building model without superstructures. This problem is made challenging since both detection and reconstruction should be performed simultaneously. Our proposed method is modular. The first stage (initialization stage) provides a fast and coarse detection of possible superstructures. The second stage (refinement stage) refines the parametric models of the coarse superstructures using either an iterative improvement scheme or a stochastic diffusion where both heuristics attempt to maximize the benefit of adding a superstructure model to the whole building model. The final stage selects the most consistent set of superstructures. Experiments as well as method comparisons show the efficiency of the proposed method.

1 INTRODUCTION

Three dimensional city models are becoming an important tool for many applications such as planning and monitoring. In recent years there has been an intensive research work to build automatic and semi-automatic systems for 3D city and building modeling (Fischer et al., 1998, Frueh and Zakhor, 2003, Kraußet al., 2007, Suveg and Vosselman, 2004, Werner and Zissermann, 2002). Despite this, there is a striking lack of works that model and reconstruct buildings with roof superstructures[1] (detailed volumes present on the roofs). This kind of modeling achieves a level of detail that finds applications in virtual or augmented reality and urban planning (Frueh and Zakhor, 2003). This level of precision impacts directly on the model realism and on the user confidence in the model quality. Current 3D city modeling algorithms consider the roof superstructures as outliers or noise that will inevitably bias their results. Very few works have addressed the detailed reconstruction of buildings. The methods presented in (Schindler and Bauer, 2003, Mayer and Reznick, 2006) have dealt with facade reconstruction containing windows.

With the availability of very high resolution aerial image-based DEMs (10cm resolution), modeling the roof superstructures becomes feasible. The data corresponding to the main roof planes are good enough to use a generic approach, but superstructures are much smaller features and their data quality can be compared to the one of entire buildings in satellite images. Generic methods have been introduced to produce free-form polyhedral building models from aerial imagery (Baillard and Zisserman, 2000, Durupt and Taillandier, 2006) but satellite data requires model-based approaches (Lafarge et al., 2007) due to their coarser resolution. Although superstructures can be described by simple parametric models, their simultaneous detection and modeling using aerial image-based DEMs could be challenging. Indeed, 1) the size of superstructures are very small compared to that of buildings, and 2) DEMs are not always a faithful representation of the real 3D world in the sense that they have some artifacts that impede fine details associated with superstructures. The context of this paper is new because the 3D-reconstruction of buildings with superstructures using very high resolution aerial images presents two different subproblems: the detection and the reconstruction.

Recently, (Brédif et al., 2007) has addressed the detection and modeling of roof superstructures. Although the proposed algorithm gives good results, its computational cost is very high since it is based on an exhaustive search strategy, in the sense that a huge number of superstructure candidates are reconstructed before selecting the optimal solution. This becomes computationally expensive whenever robust estimation techniques and/or complex superstructure types are used. In this paper, we propose an efficient approach for detecting and reconstructing roof superstructures using only a DEM. The remainder of the paper is organized as follows. Section 2 briefly describes some backgrounds and states the problem we are focusing on. Section 3 summarizes the approach described in (Brédif et al., 2007). Section 4 presents the proposed efficient technique. Section 5 provides some experimental results as well as method comparisons.

2 BACKGROUND AND PROBLEM FORMULATION

We adopt a hybrid model for buildings. This is very similar to the architectural model in (Dick et al., 2004). It allows the generic modeling of the main planes of the building with 3D-polygons, while parametric objects are used to model the smaller features that are the roof superstructures.

The **support** $supp(\mathbf{m})$ of a model $\mathbf{m}$ is simply the vertical projection of the model onto an horizontal plane. A building model is defined by $\mathcal{B} = (\mathcal{R}, \mathcal{S})$ where the roof plane set $\mathcal{R}$ defines the geometry of the 3D polygon that models each of the n roof planes, and the superstructure set $\mathcal{S}$ defines, for each roof plane $\mathcal{R}_i$, its n_i superstructures $\mathcal{S} = \mathcal{S}_{ij}$, $i \in (1 \dots n)$, and $j \in (1 \dots n_i)$, where each superstructure $\mathcal{S}_{ij}$ describes a volumetric primitive such as a chimney or a glass roof. The j^{th} **superstructure** of the roof plane $\mathcal{R}_i$ is the parametric object $\mathcal{S}_{ij} = (t_{ij}, \theta_{ij}, \phi_{ij})$ where:

- t_{ij} is one of the superstructure types that are illustrated in Figure 1. This set could be easily extended to include other superstructure types. Notice that if all superstructure types are polyhedric then the whole building model will be described by a polyhedric object.

[1] The task of superstructure modeling and reconstruction consists in estimating their type and their geometrical parameters.

- ϕ_{ij} is the set of altimetric parameters that are specific to the superstructure type, shown as the h values in Figure 1.
- $\theta_{ij} = (x_0, y_0, x_1, y_1)$ is a rectangle aligned with the principal orientation of $supp(\mathcal{R}_i)$. These parameters give the position and size of the support of $\mathcal{S}_{ij}$. For superstructure types that have rectangular supports (chimneys, glass roofs and terraces in our implementation), the rectangle defined by θ_{ij} is identical to $supp(\mathcal{S}_{ij})$.

A superstructure type t_{ij} defines hard constraints on the possible parameter values (θ_{ij}, ϕ_{ij}) of its instances. This introduces loose priors on the models. The only tight constraint is the alignment of every superstructure with the principal orientation of $supp(\mathcal{R}_i)$. This constraint does not seem to be restrictive in practice and introduces robustness in the orientation of the superstructures.

In this work, we address the following problem. Given a DEM and a building roof model without superstructures, provided by a set of 3D polygons $\mathcal{R}$, we would like to estimate the set of superstructures belonging to the building, i.e., the set $\mathcal{S}$. Therefore, there are two sub-problems: (i) the superstructure detection, and (ii) the superstructure reconstruction. In other words, we estimate for each detected $\mathcal{S}_{ij}$ its parameters (ϕ_{ij}, θ_{ij}) and its type t_{ij}.

The Z-error distance between a 3D model $\mathbf{m}$ and the DEM over the support of the superstructure $\mathcal{S}_{ij}$ is defined by

$$d_{\mathcal{S}_{ij}}(\mathbf{m}) = \sum_{supp(\mathcal{S}_{ij})} \|z_{DEM}(x,y) - z_{\mathbf{m}}(x,y)\| \qquad (1)$$

where $||.||$ is a chosen metric, and $\mathbf{m}$ is a 3D model of a superstructure or a roof plane. Note that the Z-error $d_{\mathcal{S}_{ij}}(\mathcal{S}_{ij})$ is the deviation between the DEM and the superstructure model $\mathcal{S}_{ij}$.

The benefit of adding a given superstructure $\mathcal{S}_{ij}$ to the building model will be given by:

$$e(\mathcal{S}_{ij}) = d_{\mathcal{S}_{ij}}(\mathcal{R}_i) - d_{\mathcal{S}_{ij}}(\mathcal{S}_{ij}) \qquad (2)$$

Therefore, a positive score indicates that the superstructure $\mathcal{S}_{ij}$ fits the DEM better than the roof plane $\mathcal{R}_i$. Inversely, a negative score indicates that the roof plane is a better model. Simpler models are favored using the additive description length term (Rissanen, 1978) $L(\mathcal{S}_{ij}) = L_{t_{ij}}$. The modified score can be written as:

$$e_\lambda(\mathcal{S}_{ij}) = d_{\mathcal{S}_{ij}}(\mathcal{R}_i) - d_{\mathcal{S}_{ij}}(\mathcal{S}_{ij}) - \lambda\, L(\mathcal{S}_{ij}) \qquad (3)$$

The factor λ may be set to zero when the data are of good quality. Nevertheless, setting $\lambda > 0$ may become useful to prevent overfitting with noisier data.

3 RELATED WORK

In (Brédif et al., 2007), an approach for superstructure detection and reconstruction has been proposed. The proposed optimization tries to get a set of superstructures by maximizing the sum of their scores subject to a non-overlapping constraint.

The approach consists in three steps. In the first step, feasible superstructure candidates are looked for in the 2D domain of the roof 3D polygon. For every 2D location in this quantified domain all possible 2D discrete rectangles θ_{ij} are used and tested for estimating the superstructure parameters ϕ_{ij}. In the second step, the set of superstructure candidates is filtered out using their scores, in the sense that the score of all retained superstructures is positive and local maximum. In the third step, the final set of superstructures (the solution) is found by searching for the Maximum Weighted Clique in the compatibility graph where each node corresponds to a superstructure candidate $\mathcal{S}_{ij}$ that satisfies the loose priors. The weight of the node $\mathcal{S}_{ij}$ is set to $e_\lambda(\mathcal{S}_{ij})$, and two superstructures are compatible and thus linked by an edge in the graph if they do not overlap.

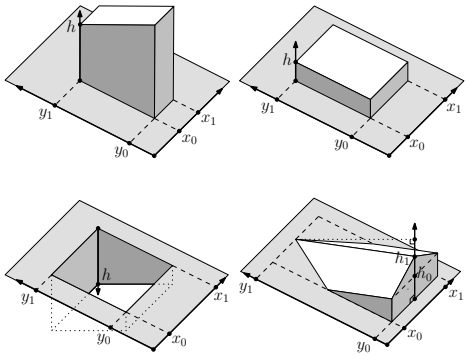

Figure 1: Four typical roof superstructures: a chimney (4+1 parameters), a terrace (4+1), a glass roof (4+1), and a dormer window (4+2).

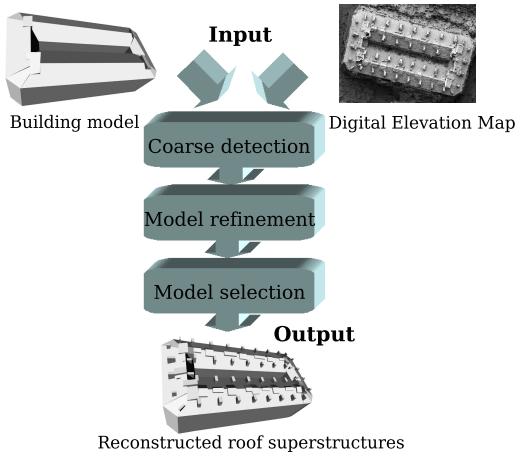

Figure 2: The three main stages of the developed approach.

While this approach provides satisfactory results, its computational cost is very high. Indeed, the reason is twofold. First, by adopting an exhaustive search strategy, a huge number of superstructure candidates are reconstructed in the first step, i.e. their model parameters ϕ_{ij} are estimated from the DEM data. The computation time associated with this first step will considerably increase when robust techniques are used for parameter estimation. Second, solving the Maximum Weighted Clique problem require processing a binary tree whose depth is $card(\mathcal{C})$ where $\mathcal{C}$ is the set of filtered superstructure candidates. While the second problem can be alleviated by using a Branch and Bound maximizer the first problem is still the bottleneck of the proposed approach.

4 EFFICIENT APPROACH

In this section, we propose an efficient approach to superstructure detection and reconstruction. The main advantage of the proposed technique is that it does not require an exhaustive search. Furthermore, its computation time is proportional to the number

of the real superstructures. The key idea is to coarsely detect the location of possible superstructures. Then, the parametric models of such superstructures is refined and validated in latter stages. Thus, the proposed approach is split into three main stages. Figure 2 outlines the proposed approach. The first stage consists in detecting and locating 3D objects able to evolve to feasible superstructures (Section 4.1). In the second stage, the set of 3D objects is then refined to a set of superstructure candidates via parameter fitting (Section 4.2). This refinement stage can use either an iterative improvement scheme or a stochastic diffusion scheme. The third stage provides the final solution as a set of non-overlapping superstructures (Section 4.3).

4.1 Coarse detection

We assume that the planes containing the 3D polygons were obtained using robust statistics such as RANSAC (Fischler and Bolles, 1981), that is, their estimation was accurate enough despite the presence of superstructures. Typically a superstructure corresponds to a set of outlier 3D points in the DEM—those 3D points that are far from the plane containing the 3D polygon. Therefore, a simple search for clusters of outliers can provide a coarse localization of possible superstructures. Every pixel belonging to the support of a 3D polygon stores the error between the DEM and the parametric model of the 3D polygon at this pixel. The obtained difference map is then thresholded using two thresholds in order to get two kinds of outliers. The lower threshold is set to the DEM noise. The upper threshold separates the pixels into low and high superstructure clusters.

Because of the nature of the DEMs used, the map of outliers will be populated with many isolated pixels and undesirable components. To eliminate them, we apply a morphological opening with a circular structuring element whose diameter is proportional to the planimetric DEM resolution. After filtering, we obtain smoothed homogeneous areas of connected pixels. Connected component labelling is then performed, which gives the number of regions used in the next stages of the algorithm. Each of these 2D regions (for example, see Figure 5**(b)**) represents an approximation of the support of a candidate superstructure.

4.2 Model refinement

We propose two algorithms for model refinement.

4.2.1 Successive improvements (algorithm I) The obtained 2D homogeneous regions are upgraded to 2D rectangles θ_k representing the support of possible superstructures. This is performed using the alignment assumption—every superstructure is aligned with the principal orientation of the support of its containing 3D polygon. At this step, due to the DEM noise and imprecision, these 2D rectangles do not necessarily correspond to the support of the real superstructures. Examples are given by i) a detected rectangle may represent a part of a glass roof (for example, see rectangles 1 and 2 in Figure 5**(c)**-upper left), and ii) a detected rectangle may be larger than the real support of a chimney (for example, see rectangle 3 in Figure 5**(c)**). In order to overcome this and to get a set of feasible superstructure candidates we adopt a fine modeling scheme by which the support and the altimetric parameters (θ_k, ϕ_k) are iteratively improved. The proposed fine modeling algorithm is illustrated in Figure 3. At any iteration, for a given type t_k and a rectangle θ_k, the estimation of the best ϕ_k^* is carried out by a classical parameter fitting that maximizes the benefit e_λ (Eq. 3). The iterative improvement (Figure 3) is carried out by locally maximizing the score $e_\lambda(t_k, \theta_k) = e_\lambda(t_k, \theta_k, \phi_k^*)$ over the parameter θ_k, for fixed type t_k.

The proposed algorithm (Figure 3) is very similar to a hill climbing maximization where the parameter space is a subset of $\mathbb{R}^4$ and the displacement vector is given by $\Delta\theta = (\delta_{x_0}, \delta_{y_0}, \delta_{x_1}, \delta_{y_1})$, where the $\delta_.$ belong to the set $\{-1, 0, +1$ quantization step$\}$.

In order to get fine delineation and reconstruction, the quantization step is set to the planimetric resolution of the DEM. One can notice that any superstructure can grow and shrink at any given iteration. In practice, due the iterative nature of the process, only 10 neighboring rectangles out of 80 are used, that is, $M = 10$. We have chosen 5 expansion directions and 5 shrinking directions. It is worth noting that, in practice, not all coarse supports require iterations since many of them are already corresponding to a local max.

Model refinement: successive improvements

Input: a list of 2D rectangles θ_k provided by the coarse detection stage.
Output: a list of superstructure candidates $\mathcal{C}_i = (\mathcal{S}_{ij}), j \in (1 \dots n_i)$.

For every detected 2D rectangle θ_k and for all its associated feasible types t_k, do the following

1. Compute the scores $e_\lambda(t_k, \theta_k + \Delta\theta_m)$ for the neighboring rectangles $(\theta_k + \Delta\theta_m)$, $m = 1 \dots M$.
2. If the current superstructure (t_k, θ_k, ϕ_k) is a local maximum, that is, $e_\lambda(t_k, \theta_k) \geq e_\lambda(t_k, \theta_k + \Delta\theta_m)$ for all m or the support of any neighboring rectangle exceeds its allowed boundaries then add the current superstructure (t_k, θ_k, ϕ_k) to the set of superstructure candidates and stop the iterations.

   Otherwise replace the so far best superstructure (t_k, θ_k, ϕ_k) with the neighbor having the highest score, i.e., $(t_k, \theta_k, \phi_k) \leftarrow (t_k, \theta_k + \Delta\theta_{m^*}, \phi_{m^*})$ where m^* is the neighbor having the highest score. Go to (1).

Figure 3: The refinement algorithm upgrades the coarse 2D supports to feasible 3D superstructure models by locally maximizing their score e_λ.

Model refinement: stochastic diffusion

Input: a list of 2D rectangles θ_k provided by the coarse detection stage.
Output: a list of superstructure candidates $\mathcal{C}_i = (\mathcal{S}_{ij}), j \in (1 \dots n_i)$.

For every detected 2D rectangle θ_k and for all its associated feasible types t_k, do the following

1. Compute the scores $e_\lambda(t_k, \theta_l)$ for the neighboring rectangles ($l = 1 \dots L$). The neighboring rectangles θ_l are drawn using uniform distributions.
2. Replace the current superstructure (t_k, θ_k, ϕ_k) with the superstructure having the highest score, i.e., $(t_k, \theta_k, \phi_k) \leftarrow (t_k, \theta_{l^*}, \phi_{l^*})$ where l^* is the superstructure having the highest score.

Figure 4: The refinement algorithm upgrades the coarse 2D supports to feasible 3D superstructure models by means of stochastic diffusion.

4.2.2 Stochastic diffusion (algorithm II) The refinement algorithm presented above upgrades the coarse supports to superstructure 3D models by searching for local maxima of the scores. In this section, we propose an alternative refinement algorithm that is based on a stochastic diffusion. In other words, for each coarse support and each type, the coarse support is diffused using a given number of drawn rectangles. Since the 2D orientation is already known, every drawn rectangle requires drawing four continuous random variables (width, length, and 2D position). We have used uniform distributions to get such rectangles. The range of widths and lengths is set to the type range. The 2D position is limited to keep the center of the detected coarse rectangle in the drawn rectangle. The score of all drawn supports is then computed. The selected candidate is the one having the highest score. Figure 4 outlines this algorithm. Although this algorithm is very similar to the previous algorithm, the iterative step is replaced with a stochastic diffusion step (one single pass). The number of drawn rectangles L was experimentally determined. It was set to 60.

The main advantage of the stochastic diffusion scheme is its ability to escape non-desired local maxima since the search for 2D supports is performed at random.

4.3 Final solution

The output of the refinement algorithm is a set of superstructures that may overlap. Thus, the final step consists in selecting a set of non-overlapping superstructures whose sum of scores is maximum. This is the maximum Weighted Clique problem. The final set of non-overlapping superstructures is derived from the set of superstructure candidates $\mathcal{C}_i$ by maximizing their total scores.

$$\underset{\mathcal{S}_{ij} \subset \mathcal{C}_i}{argmax} \sum_j e_\lambda(\mathcal{S}_{ij})$$

subject to $supp(\mathcal{S}_{im}) \cap supp(\mathcal{S}_{in}) = \emptyset$ where $\mathcal{S}_{in}, \mathcal{S}_{im} \in \mathcal{C}_i$. In our case, since the number of superstructure candidates that overlap with at least one superstructure is very small, the Maximum Weighted Clique problem can be solved using a brute force exploration.

5 EXPERIMENTAL RESULTS

Results have been obtained from DEMs and polyhedric building models developed at the French Geographical Institute (IGN). The DEMs have been obtained from a set of calibrated aerial images using the graph cut algorithm (Roy and Cox, 1998). The DEM-produced building model (a set of 3D polygons) have been obtained using the generic reconstruction method (Durupt and Taillandier, 2006). As a result the input data are given by the DEM only, the images are not used directly.

We have implemented the $\mathcal{L}^1$ and $\mathcal{L}^2$ metrics. The $\mathcal{L}^1$ metric is more adapted to non-Gaussian noise typically affecting correlation-based DEMs, but the computation time of the latter is much faster. Figure 5 illustrates the application of the proposed approach to a typical building roof. **(a)** shows the orthophoto of the corresponding 3D polygon. **(b)** shows the results of the coarse detection scheme—a set of connected regions, **(c)** shows the initial and coarse supports, **(d)** shows the result of applying the iterative fine modeling scheme (the set of refined superstructures $\mathcal{C}_i$), **(e)** shows the selected non-overlapping superstructures, **(f)** shows the roof model with the reconstructed superstructures. We stress the fact that the orthophoto was not used by the proposed algorithms. It is only used for visualization and validation purposes.

Figure 6 shows the score evolution associated with two coarse supports of Figure 5**(c)** (rectangles 1 and 2). These two coarse supports represent a fragment of the same upper left superstructure. Iteration 0 corresponds to the score of the coarse support and the final iteration corresponds to the obtained local maximum. One can notice that both supports have converged to roughly the same superstructure (see Figure 5**(d)**-upper left). Figure 7 shows the score evolution associated with another coarse support (rectangle 3). The lower part of this figure shows the coarse support (left) and the support obtained at convergence (right).

For comparison purposes, the DEM data associated with the roof shown in Figure 5 were processed by the exhaustive search-based method (Brédif et al., 2007). The detection results are shown in Figure 8. As can be seen, the detection of chimneys was almost the same for both approaches. However, the detected low superstructures were not the same although their overall detection rates were almost the same (see Figure 5**(e)**).

Figure 9 shows the results of roof superstructure reconstruction using our proposed method based on stochastic diffusion. Figure 10 shows another result of roof superstructure reconstruction.

Method comparison. In addition to the comparison provided by Figures 5**(e)** and 8, we have compared the performance of three approaches. Figure 11 shows the superstructure detection results associated with another typical building roof: **(a)** corresponds to the exhaustive search-based method (Brédif et al., 2007), **(b)** to the proposed approach based on successive improvements, and **(c)** to the proposed approach based on stochastic diffusion. As can be seen, the detection results obtained with the proposed approaches (Section 4) are very similar to those obtained with the exhaustive search-based method. However, the proposed approach is much faster (see Table 1). It should be noticed that some glass roofs were not detected by any method. This under-detection is due to the difficulty to separate the imperfections of the DEM from the glass roof models which have very small height. The rightmost chimneys were not detected by our proposed method since their size (within the building footprint) was smaller than the size of the opening operator. Furthermore, by comparing **(b)** and **(c)** one can notice that the method based on the successive improvements has provided very good delineation of the 2D supports. This is due to the iterative process by which the 2D support is estimated by locally maximizing a score in the parameter space $\mathbb{R}^4$. On the other hand, the stochastic diffusion scheme explores the parameter space at random. However, the stochastic diffusion scheme can be very useful in cases when the DEM noise is significant.

Computation time. Table 1 summarizes the CPU time associated with the typical building shown in Figure 11. The first column corresponds to the exhaustive search-based method (Brédif et al., 2007). The second column corresponds to the method based on successive improvements. The third column corresponds to the method based on stochastic diffusion. The first row corresponds to the $\mathcal{L}^2$ metric-based parameter fitting, and the second row to the $\mathcal{L}^1$ metric-based parameter fitting. An Intel Xeon 1.6 GHz PC with a non-optimized C++ code has been used.

In general, the CPU time of the exhaustive search-based method is proportional to the building size, whereas the CPU time of our proposed approach is proportional to the number of the real superstructures.

6 CONCLUSION

We presented an efficient and modular approach for reconstructing building superstructures using only a DEM, an initial building

(a)

(b)

(c)

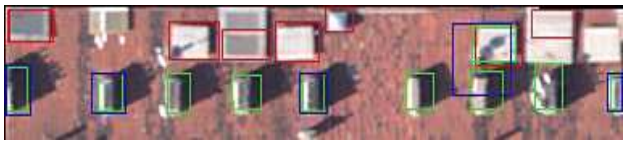

(d)

(e)

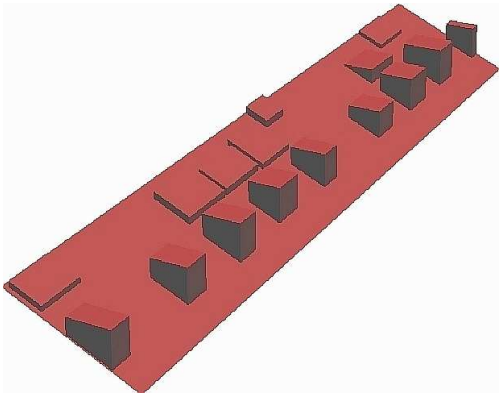

(f)

Figure 5: **(a)** The orthophoto. **(b)** The connected regions obtained by clustering outlier points. **(c)** The initial and coarse 2D rectangles/supports. **(d)** The superstructure candidates obtained by iterative improvements. **(e)** The selected set of superstructures. **(f)** The final roof 3D model.

	(Brédif et al., 2007)	*Succ. improv.*	*Stoch. diffusion*
$\mathcal{L}^2$ metric	49 s	3.5 s	10.5 s
$\mathcal{L}^1$ metric	67 s	7.1 s	14.3 s

Table 1: Computational time associated with the building shown in Figure 11.

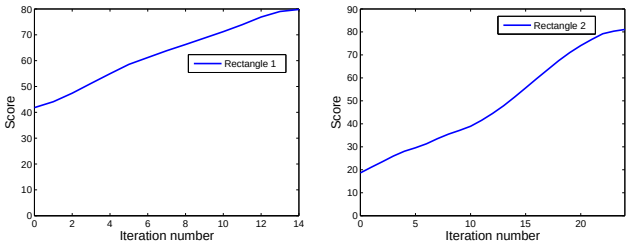

Figure 6: The score evolution as a function of the iteration number associated with the two rectangles shown in Figure5**(c)** (the upper left corner). Iteration 0 corresponds to the coarse support and the final iteration corresponds to a local maximum. One can notice that both supports have converged to the same superstructure (see Figure 5**(d)**).

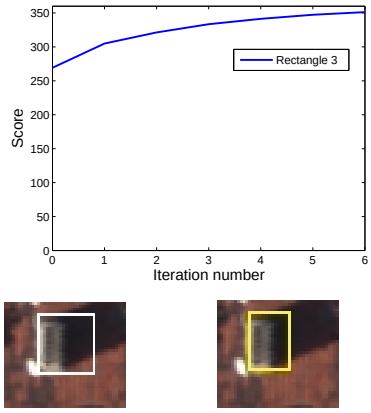

Figure 7: The score evolution as a function of the iteration number associated with the coarse rectangle (bottom-left).

Figure 8: The detected and reconstructed superstructures using the exhaustive search-based method.

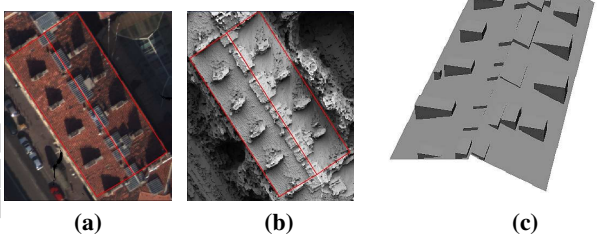

(a) **(b)** **(c)**

Figure 9: **(a)** The orthophoto. **(b)** A shaded view of the DEM. **(c)** The detected and reconstructed superstructures.

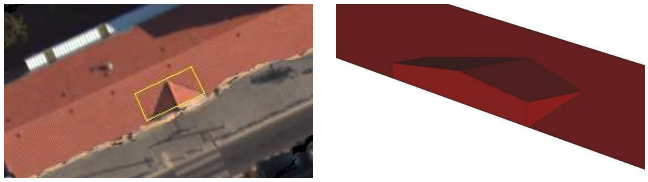

Figure 10: **(a)** The orthophoto. **(b)** The detected and reconstructed superstructure.

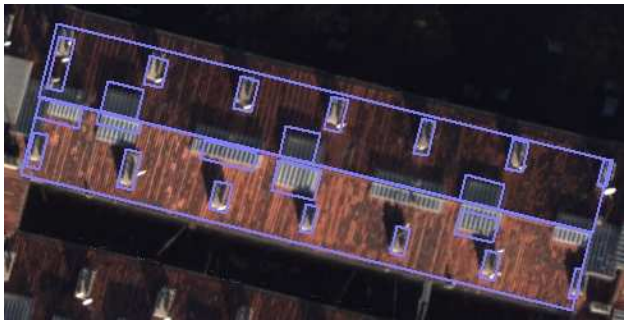

(a)

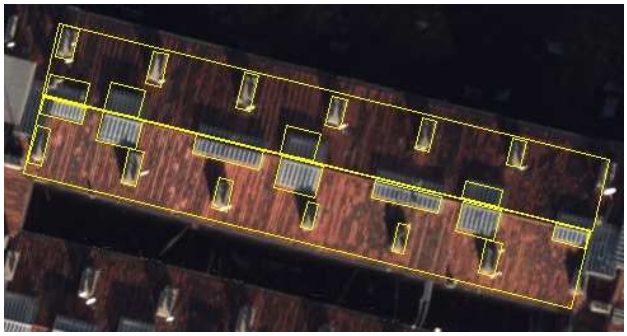

(b)

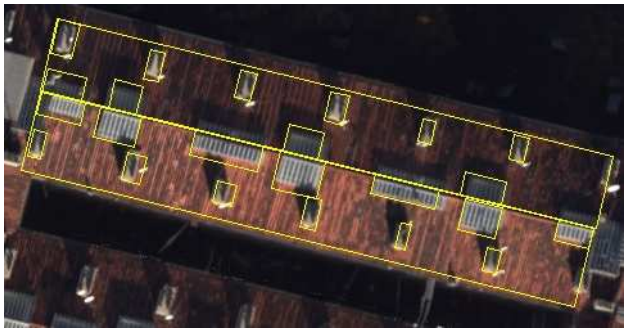

(c)

Figure 11: Detecting and reconstructing superstructures associated with a typical building roof. **(a)** results obtained with the exhaustive search-based method. **(b)** results obtained with the proposed approach based on successive refinements. **(c)** results obtained with the proposed approach based on stochastic diffusion.

model without superstructures and an easily extensible collection of parametric models defining the available superstructure types. The approach consists of three main stages. In the first stage, possible superstructures are roughly detected using the DEM and a polyhedric building model. In the second stage, the superstructure parametric models are estimated using either successive improvements or a stochastic diffusion. The final stage selects the most consistent set of superstructures. The computational time of the proposed approach is proportional to the number of real superstructures. Several comparisons with an exhaustive search based approach show that the approach give similar results. Although determining the type of the reconstructed superstructures was a by-product of the proposed approach our main objective was the detection and reconstruction of the superstructures. Future work may investigate the superstructure reconstruction directly from the images.

REFERENCES

Baillard, C. and Zisserman, A., 2000. A plane-sweep strategy for the 3D reconstruction of buildings from multiple images. In: 19th ISPRS Congress and Exhibition.

Brédif, M., Boldo, D., Pierrot-Deseilligny, M. and Maître, H., 2007. 3D building reconstruction with parametric roof superstructures. In: IEEE International Conference in Image Processing.

Dick, A., Torr, P. and Cipolla, R., 2004. Modelling and interpretation of architecture from several images. International Journal of Computer Vision 60(2), pp. 111–134.

Durupt, M. and Taillandier, F., 2006. Automatic building reconstruction from a digital elevation model and cadastral data: an operational approach. In: Proc. ISPRS Photogrammetric Computer Vision, ISPRS.

Fischer, A., Kolbe, T., Felicitas, L., Cremers, A., Forstner, W., Plumer, L. and Steinhage, V., 1998. Extracting buildings from aerial images using hierarchical aggregation in 2D and 3D. Computer Vision and Image Understanding.

Fischler, M. and Bolles, R., 1981. Random sample consensus: A paradigm for model fitting with applications to image analysis and automated cartography. Communication ACM 24(6), pp. 381–395.

Frueh, C. and Zakhor, A., 2003. Constructing 3D city models by merging ground-based and airborne views. In: IEEE Computer Vision and Pattern Recognition.

Krauß, T., Reinartz, P. and Stilla, U., 2007. Extracting orthogonal building objects in urban areas from high resolution stereo satellite image pairs. In: ISPRS Photogrammetric Image Analysis.

Lafarge, F., Descombes, X., Zerubia, J. and Pierrot-Deseilligny, M., 2007. 3D city modeling based on Hidden Markov Model. In: IEEE International Conference in Image Processing.

Mayer, H. and Reznick, S., 2006. MCMC linked with implicit shape models and plane sweeping for 3D building facade interpretation in image sequences. In: Proc. ISPRS Photogrammetric Computer Vision.

Rissanen, J., 1978. Modeling by shortest data description. Automatica 14, pp. 465–471.

Roy, S. and Cox, I., 1998. A maximum-flow formulation of the n camera stereo correspondence problem. In: IEEE International Conference on Computer Vision.

Schindler, K. and Bauer, J., 2003. A model-based method for building reconstruction. In: IEEE International Workshop on Higher-Level Knowledge in 3D Modeling and Motion Analysis.

Suveg, I. and Vosselman, G., 2004. Reconstruction of 3D models from aerial images and maps. ISPRS Journal of Photogrammetry and Remote Sensing 58(3-4), pp. 202–224.

Werner, T. and Zissermann, A., 2002. New techniques for automated architectural reconstruction from photographs. In: European Conference on Computer Vision.